Acta Crystallographica Section D
Biological Crystallography
ISSN 0907-4449

Design, X-ray crystallography, molecular modelling and thermal stability studies of mutant enzymes at site 172 of 3-isopropylmalate dehydrogenase from *Thermus thermophilus*

Chunxu Qu,[a] Satoshi Akanuma,[a] Nobuo Tanaka,[a]* Hideaki Moriyama[a] and Tairo Oshima[b]

[a]Department of Life Science, Graduate School of Bioscience and Biotechnology, Tokyo Institute of Technology, Nagatsuta 4259, Yokohama 226-8501, Japan, and [b]Department of Molecular Biology, Tokyo University of Pharmacy and Life Science, Horinouchi 1432-1, Hachioji, Tokyo 192-0392, Japan

Correspondence e-mail: ntanaka@bio.titech.ac.jp

Received 3 August 2000
Accepted 13 November 2000

PDB References: A172F, 1gc8; A172G, 1gc9; A172V, 1g2u.

The relationship between the structure and the thermostability of the 3-isopropylmalate dehydrogenase from *Thermus thermophilus* was studied by site-directed mutation of a single Ala residue located at the domain interface. The crystal structures of three mutant enzymes, replacing Ala172 with Gly, Val and Phe, were successfully determined at 2.3, 2.2 and 2.5 Å resolution, respectively. Substitution of Ala172 by relatively 'short' residues (Gly, Val or Ile) enlarges or narrows the cavity in the vicinity of the C^{β} atom of Ala172 and the thermostablity of the enzyme shows a good correlation with the hydrophobicity of the substituted residues. Substitution of Ala172 by the 'longer' residues Leu or Phe causes a rearrangement of the domain structure, which leads to a higher thermostability of the enzymes than that expected from the hydrophobicity of the substituted residues. Mutation of Ala172 to negatively charged residues gave an unexpected result: the melting temperature of the Asp mutant enzyme was reduced by 2.7 K while that of the Glu mutant increased by 1.8 K. Molecular-modelling studies indicated that the glutamate side chain was sufficiently long that it did not act as a buried charge as did the aspartate, but instead protruded to the outside of the hydrophobic cavity and contributed to the stability of the enzyme by enhancing the packing of the local side chains and forming an extra salt bridge with the side chain of Lys175.

1. Introduction

It is difficult to correctly predict the three-dimensional structure of a protein based on its amino-acid sequence, because how the protein folds, the kinds of forces involved and how the forces affect the stability of protein conformation remain obscure.

The role of hydrophobic interactions in stabilizing folded proteins has been extensively studied by site-directed mutagenesis of the α-subunit of tryptophan synthase (Yutani *et al.*, 1987), barnase (Kellis *et al.*, 1988, 1989), T4 lysozyme (Matsumura *et al.*, 1988, 1989; Daopin, Alber *et al.*, 1991; Hurley *et al.*, 1992; Eriksson *et al.*, 1992), human lysozyme (Takano *et al.*, 1995), l-repressor protein (Lim & Sauer, 1991), gene V protein from bacteriophage f1 (Sandberg & Terwilliger, 1989; Zhang *et al.*, 1996), staphylococcal nuclease (Shortle *et al.*, 1990), ribonuclease HI from *Escherichia coli* (Ishikawa *et al.*, 1993), α-amylase from *Bacillus licheniformis* (Declerck *et al.*, 1995) and 3-isopropylmalate dehydrogenase (Moriyama *et al.*, 1995; Sakurai *et al.*, 1995). The contribution of hydrophobicity to protein stability has been well summarized by Baldwin & Matthews (1994). Furthermore, studies of multiple amino-acid replacements at a single site (Yutani *et al.*,

1987; Matsumura *et al.*, 1988; Declerck *et al.*, 1995) have shown that the contribution of an amino acid to protein stability is proportional to the corresponding free energy required to transfer the amino acid from water to organic solvent. However, in such cases, some residues deviated considerably from the correlation line and Yutani *et al.* (1987) pointed out that the protein stabilities

> tended to increase linearly with increasing hydrophobicity of the substituted residue, unless the volume of the substituted residue was over a certain limit.

A leucine biosynthetic enzyme, 3-isopropylmalate dehydrogenase (IPMDH; *threo*-D-3-isopropylmalate NAD^+ oxidoreductase; E.C. 1.1.1.85), from an extreme thermophile, *T. thermophilus*, is more thermostable than that from *B. subtilus*. To gain some insight into the mechanism involved in the stabilization of IPMDH from *T. thermophilus*, various chimeric enzymes (Onodera *et al.*, 1994; Numata *et al.*, 1995) have been created and investigated. One of the chimeric enzymes, 2T2M6T, was produced by replacing the amino-acid sequence of the enzyme from *T. thermophilus* (hereafter referred to as 10T) from residues 75–133 by the corresponding part of the mesophilic enzyme from *B. subtilus* (hereafter referred to as 10M). One thermostable mutant, 2T2M6T-A172V, was generated evolutionally by cultivating the clone at 349 K (Kotsuka *et al.*, 1996). The mutation site, Ala172, is on the *T. thermophilus* part; therefore, the same mutation A172V was introduced into 10T, by which the enzyme was found to be further stabilized. Furthermore, a similar evolutionary experiment produced another thermostable mutant 2T2M6T-A172L using 2T2M6T-A172S as the starting molecule for directed evolution. Introduction of leucine at position 172 of the *T. thermophilus* enzyme also further improved the thermal stability of the inherent thermostable enzyme (Akanuma *et al.*, 1995). It was suggested that the residue in this site contributes to the thermostability by increasing the hydrophobic interactions. However, the structural analysis of the mutant enzyme 10T-A172L showed that the arrangement of domain structure was different from that of 10T (Qu *et al.*, 1997). Several single-mutant enzymes at site 172 were constructed and their structural studies were undertaken in order to elucidate the mechanism of thermal stability of these mutant enzymes, as well as the mechanism of domain movement found in the A172L mutant enzyme.

The structure of IPMDH from *T. thermophilus* has been determined (Imada *et al.*, 1991). As described by Qu *et al.* (1997), Ala172 is located on the interface of two domains and is a buried residue on the C-terminal α-helix. A rigid hydrophobic cavity exists around its C^{β} atom. In the present study, we mutated Ala172 to seven other amino acids, taking their hydrophobicities, α-helical propensities and side-chain sizes into consideration. Their melting temperature obtained by CD measurement and their structures obtained by either X-ray crystallography or molecule modelling indicated how the hydrophobic interactions around site 172 contribute to the overall stability of the protein and also how well the structure accommodates the mutation by self-adjustment. Other factors affecting protein stability, such as local propensity and hydrogen bonds or salt bridges, are also discussed (Dill, 1990).

Table 1
Crystallographic data and data-collection statistics of A172V, A172G and A172F.

All experiments were undertaken at room temperature with the R-AXIS IIc.

	A172V	A172G	10T†	A172F	A172L‡
Crystal system	Trigonal	Trigonal	Trigonal	Monoclinic	Monoclinic
Space group	$P3_221$	$P3_221$	$P3_221$	$P2_1$	$P2_1$
Unit-cell parameters					
a (Å)	78.68 (1)	78.61 (1)	78.6	55.255 (6)	55.6
b (Å)				87.830 (8)	88.1
c (Å)	157.69 (2)	158.06 (2)	158.1	71.186 (8)	72.0
β (°)				100.02 (7)	100.9
Nz§	6	6	6	4	4
Resolution limit (Å)	2.1	2.3	—	2.5	—
Completeness (%)	89.4	88.5	—	92.8	—
$R_{\rm merge}$¶ (%)	5.83	6.38	—	5.58	—
Consistency factor†† (%)	5.5	6.5	—	9.6	—

† See Imada *et al.* (1991) for details. ‡ See Qu *et al.* (1997) for details. § The number of subunits in the unit cell. ¶ Reliability factor among symmetry-equivalent reflections. $R_{\rm merge} = \sum|I_i/G_i - \langle I_i\rangle|)/\sum\langle I_i\rangle$, where I_i is one of the intensities of reflection that can be related to a symmetry operation, G_i is a scale factor and $\langle I_i\rangle$ is the average of I_i/G_i. †† Consistency factor = $(\sum|F_1| - |F_2|)/\sum\langle F\rangle$, where $\langle F\rangle = (|F_1| + |F_2|)/2$ and F_2 was scaled to F_1 according to the Wilson plot.

2. Materials and methods

Construction and purification of some mutant enzymes have been reported previously (Kotsuka *et al.*, 1996; Akanuma *et al.*, 1997). The base substitutions corresponding to Ala172→Gly, Ile and Phe were introduced into the *T. thermophilus leuB* gene according to the method of Kunkel *et al.* (1987). Oligonucleotides used for generating the mutations were 5′-CTG CGC TTC CTG GCG CCC TCA AAG GCC A-3′ (Ala→Gly), 5′-CG CTT CCT CGC GAT TTC GAA GGC CAC CCG-3′ (Ala→Ile) and 5′-CGC TTC CTC GCG AAT TCA AAG GCC ACC-3′ (Ala→Phe). The mutations in the gene were confirmed by nucleotide sequencing. The wild-type and mutant enzymes were overproduced in *E. coli* JA221 harbouring the respective expression plasmids and purified as described by Yamada *et al.* (1990). Each enzyme was confirmed to be homogeneous as judged by SDS–gel electrophoresis. Thermal denaturation of each purified enzyme was measured with a JASCO J720C spectropolarimeter. To prevent aggregate formation after denaturation, the circular dichroism (CD) measurements were carried out in an alkaline buffer. The enzymes were dissolved in 20 m*M* $NaHCO_3$ (pH 10.9); the enzyme concentration was 0.2 mg ml^{-1}. The temperature of the enzyme solution was controlled with a circulating bath and a programmable temperature controller. The precise temperature was monitored with a thermocouple and the scan rate was 1.0 K min^{-1}. The thermal denaturation curves were normalized as described by Iwasaki *et al.* (1996). The catalytic activity of the enzymes was determined as described in Qu *et al.* (1997).

Table 2
Statistics of structural refinement of A172V, A172G and A172F mutants.

Structural refinement	A172V	A172G	A172F
Resolution (Å)	6.0–2.2	6.0–2.3	10.0–2.5
No. of reflections used	21122	16105	20506
R factor† (%)	17.9	17.9	17.8
No. of water molecules	67	55	73
R.m.s. deviation of bond length (Å)	0.006	0.007	0.007
R.m.s. deviation of bond angle (°)	1.341	1.387	1.334
Ramachandran plot statistics (%)			
Most favoured region	91.8	90.0	90.4
Additional allowed region	7.8	9.3	9.0
Generously allowed regions	0.4	0.7	0.5
Disallowed regions	0.0	0.0	0.0

† *R* factor is defined as $\sum ||F_{obs}| - |F_{calc}|| / \sum |F_{obs}|$.

2.1. Crystallization and collection of diffraction data

Crystals of A172G and A172V were obtained under the same crystallization conditions as the wild-type enzyme (Sakurai *et al.*, 1992). Crystals of dimensions 0.3 × 0.3 × 0.7 mm were used for data collection on a Rigaku R-AXIS IIc diffractometer (Sato *et al.*, 1992). The crystals belong to space group $P3_221$, with unit-cell parameters a = 78.61 (1), c = 158.06 (2) Å for A172G and a = 78.68 (1), c = 157.69 (2) Å for A172V; both crystals are isomorphous with the trigonal crystal of 10T. There is one subunit per asymmetric unit and V_M is 3.7 Å^3 Da^{-1} in both cases. A summary of data collection and statistics is given in Table 1.

As was the case for the A172L enzyme, the A172F enzyme could not be crystallized by the salting-out technique with ammonium sulfate (Sakurai *et al.*, 1992). The crystal was obtained at pH 4.8 using polyethylene glycol 4000 (PEG 4K) as a precipitant. The protein was dissolved in 20 m*M* potassium phosphate buffer pH 7.6. The reservoir solution was 2% PEG 4K dissolved in 0.1 *M* sodium acetate buffer pH 4.8. A 5 µl aliquot of 10 mg ml^{-1} protein solution was mixed with 5 µl reservoir solution on the cover slip. Crystals with three or four lobes grew at 298 K after a week. One lobe, with dimensions of 0.25 × 0.25 × 0.4 mm, was used for data collection. The crystal of the A172F enzyme belongs to the monoclinic system, space group $P2_1$, with unit-cell parameters a = 55.26 (2), b = 87.83 (2), c = 71.19 (3) Å, β = 100.0 (3)°, and is isomorphous to the crystal of A172L. There is one dimer per asymmetric unit and V_M is 2.4 Å^3 Da^{-1}. A summary of the data collection and statistics is given in Table 1.

Crystals of the A172E mutant enzyme were obtained from a drop equilibrated with reservoir solution consisting of 0.8 *M* ammonium sulfate pH 6.0 at either 288 or 293 K. There are two types of crystals: one is hexagonal bipyramidal (type I) and the other is tetragonal (type II). Type I crystals appear earlier than type II crystals but easily transform to type II; as time passes, many thin slices of type II are inserted into the hexagonal type I crystal. Although type I crystals of dimensions 0.3 × 0.3 × 0.7 mm with a shiny surface were used for data collection, the crystals only diffracted to 7 Å using the laboratory facility and to 5 Å using synchrotron radiation. The Patterson symmetry of the crystals was *P*4/*mmm*, with unit-cell parameters $a = b$ = 145.1, c = 64.5 Å, or *Pmmm*, with unit-cell parameters a = 145.3, b = 144.9, c = 64.3 Å.

2.2. Determination and refinement of structures

The molecular-replacement method was applied to the structural analysis of all three mutant enzymes using the program *X-PLOR* (Brünger *et al.*, 1990). The structure of the wild-type enzyme was chosen as the initial model for the structure determination of A172V and A172G, and the structure of A172L was chosen for the A172F mutant. The slow-cooling protocol was applied after the molecular orientation was refined with the rigid-body refinement in each case. Mutation at site 172, replacing Ala with Val, Gly or Phe, and model modification was achieved using the *FRODO* program (Jones, 1985). The final *R* factors of A172V, A172G and A172F were 17.9, 17.9 and 17.8%, respectively. The detailed structural refinement statistics are listed in Table 2.

2.3. Molecular modelling

Molecular modelling of A172E and A172D was performed on an Indigo II machine using the *QUANTA*/*CHARMM* (MSI) system. The wild-type structure was used as the initial

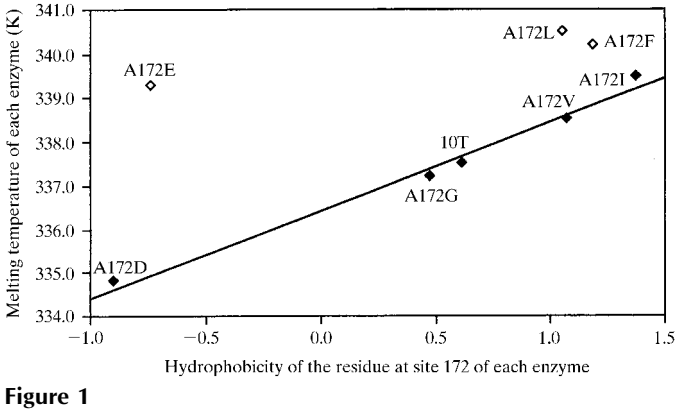

Figure 1
The correlation between the enzyme stability and the hydrophobicity of the residue at site 172. Only the mutant enzymes represented by filled symbols are used for the calculation of the least-squares fitting line.

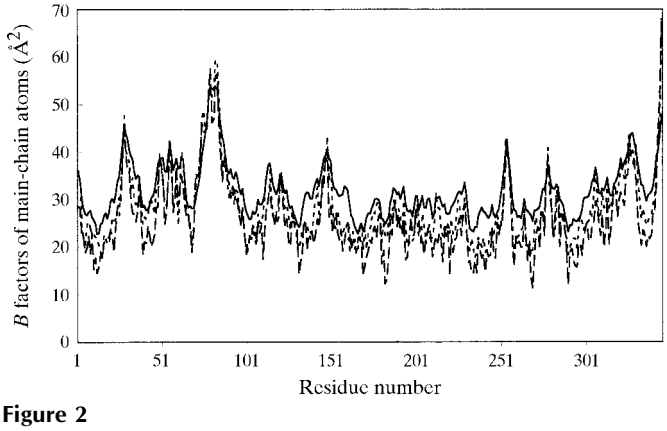

Figure 2
The distribution of temperature factors of main-chain atoms. The solid line, dotted line and dashed line represent wild-type enzyme, A172V and A172G, respectively.

model. Ala172 was replaced with Glu or Asp, respectively, and the new side chains were adjusted using the 'Spin' side-chain module in the 'Model' side-chain palette of the 'Protein Design' utility of *QUANTA*. Initially, the local structures were minimized for 200 steps using the steepest descents algorithm and were then minimized using the adopted-basis Newton–Raphson algorithm until the system converged with the program *CHARMM*. Atom constraints was used in all processes. All atoms outside the 6 Å sphere centred at residue 172 were fixed and the inside atoms were tethered with a force constant of 100 kcal $Å^{-1}$ mol^{-1} (1 kcal = 4.184 kJ), while the mutation site was totally free.

3. Results

3.1. The design of mutant residues

In the wild-type structure, the residue at 172 is totally buried. Assuming that it is exposed to the solvent in the unfolded state, its contribution to protein stability should be proportional to the energy of transfer of the residue from water to organic solvent. Therefore, we designed a series of mutant enzymes, each of which has a side chain of a different size and hydrophobicity. All the mutant enzymes were named after their replaced residues, while the wild-type enzyme was designated as 10T. Considering the conformation of Ala172 in the wild-type structure, it was thought that a residue with a higher α-helix-forming propensity would produce little disruption to the local structure. With the exception of Gly, all the other replaced residues have a similar α-helix-forming propensity to Ala, which implies that Gly might decrease the thermostability of the mutant enzyme more than expected.

3.2. Thermostability and activity

All the variant enzymes listed in Table 3 were purified and their relative activities and mid-points of thermal unfolding curve (Tm) were measured by monitoring the change in ellipticity at 222 nm in the alkaline buffer. All the variant enzymes have similar activities to the wild-type enzyme and the more hydrophobic the replacing residue, the higher the Tm of the mutant. As shown in Fig. 1, a clear correlation was observed between the hydrophobicity of the residue and the thermostability of the enzyme. However, three mutant enzymes, substituted by Leu, Phe and Glu, deviated from the linearity towards higher thermostability. Individual reasons for excess of thermostability for each residue will be discussed later.

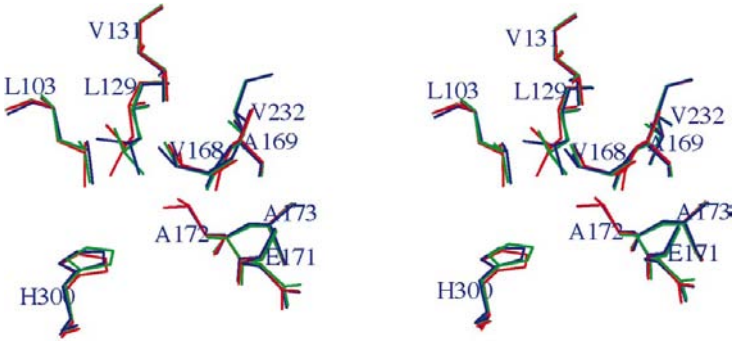

Figure 3
Superimposed local structures of the mutant enzymes A172G (green lines) and A172V (red lines) on the wild-type enzyme (blue lines). This figure was drawn using *MOLSCRIPT* (Kraulis, 1991).

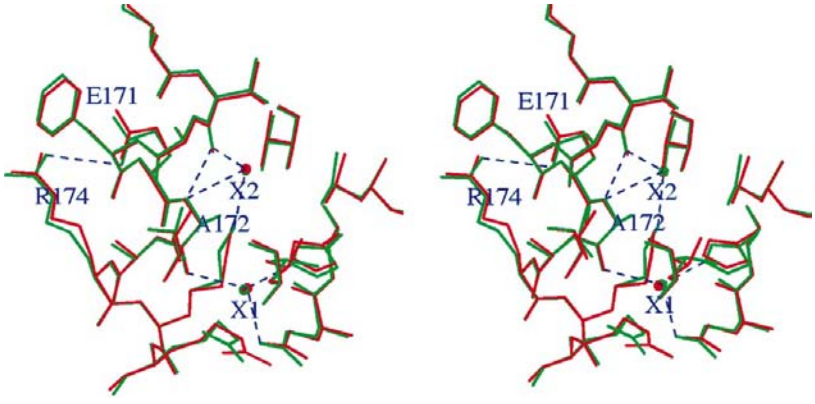

Figure 4
Two conserved water molecules (X1 and X2) around the mutation site. The green lines represents the wild-type enzyme and the red lines represents the mutant A172G. X1 is hydrogen bonded to 172 O, 299 $O^{\delta2}$ and 300 $N^{\delta2}$. X2 is hydrogen bonded to 168 O, 172 N and 175 N^{ζ}. There is a salt bridge between residues Glu171 and Arg174. This figure was drawn using *MOLSCRIPT* (Kraulis, 1991).

3.3. Crystal structure of A172V and A172G

The structures of the two mutant enzymes A172V and A172G are similar to that of the wild-type enzyme. The root-mean-square deviations of C^{α} atoms from 10T are 0.18 Å for A172V and 0.19 Å for A172G. The temperature-factor distributions of the two structures are also similar to that of 10T, as shown in Fig. 2.

Fig. 3 shows the superimposed local structures of A172V, A172G and 10T. All three structures are very similar except for the side chains of two residues, Leu129 and His300. The mutation site is located on the large α-helix; the positions of the C^{α} and C^{β} atoms were constrained by the main chain not to be greatly changed. In the case of the A172G structure, in order to fill the vacant space in the cavity, the C^{γ} atom and one of C^{δ} atoms of Leu129 moved into the cavity by rotation of the $C^{\alpha}-C^{\beta}$ and $C^{\beta}-C^{\gamma}$ bonds; the ring of His300 also moved towards the C^{α} atom of Gly172 by rotation of the $C^{\alpha}-C^{\beta}$ bond. In contrast, the opposite tendency was manifested in the case of the A172V mutant structure. The side chain of Leu129 rotated outwards and the ring of His300 was shifted away from the side chain of Val in order to prevent short van der Waals contacts.

The peptide segment including Ala172 is shown in Fig. 4. Residues 159–173 form one

Table 3
The relative activity and the melting temperature for all the variant enzymes studied.

The activities were measured at 333 K in 100 m*M* potassium phosphate pH 7.6 containing 1 *M* KCl, 20 m*M* $MnCl_2$, 800 m*M* NAD and 800 m*M* D,L-IPM. The melting temperature (Tm) was determined at pH 10.9 by the circular dichroism measurement. ΔTm is the difference between the Tm values of the mutant enzyme and the wild-type enzyme. The same results were obtained from at least three independent measurements.

Enzyme	Relative activity	Tm (K)	ΔTm (K)
10T	1.0	337.5	—
A172V	1.1	338.5	+1.0
A172I	1.1	339.5	+2.0
A172L	1.1	340.5	+3.0
A172F	0.84	340.2	+2.7
A172G	1.0	337.2	−0.3
A172D	0.94	334.8	−2.7
A172E	1.0	339.3	+1.8

helix, while residues 174–178 form a 5-turn [CO(*I*)···HN(*I* + 4)] with a salt bridge between the side chains of Gly171 and Arg174 (Fig. 4). Ala172 NH is hydrogen bonded to Val168 CO, while Ala172 CO is loosely hydrogen bonded to Lys175 NH. Both Ala172 NH and Ala172 CO are also hydrogen bonded to water molecules which were conserved in the structure of A172G (Fig. 4). Therefore, with the help of the water molecule and one salt bridge across the mutation site, the local structure in the mutant enzyme A172G is not disrupted. However, neither of the two water molecules were found in the structure of A172V. The present observations were also found in the mutations of human lysozyme (Takano, Funasaki *et al.*, 1997).

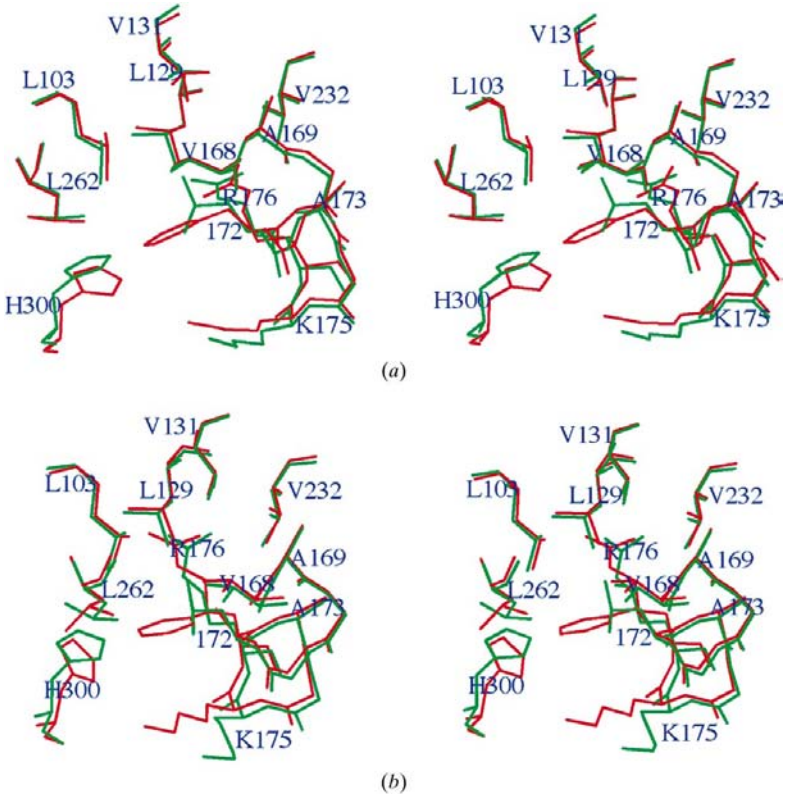

Figure 5
Superimposed local structures of the mutant enzyme A172F (green lines) on A172L (red lines). (*a*) and (*b*) represent the two subunits. This figure was drawn using *MOLSCRIPT* (Kraulis, 1991).

3.4. Crystal structure of A172F

The structure of the A172F mutant enzyme is very similar to that of the A172L mutant enzymes. Two monomers exist in the asymmetric unit. A dimer is composed of two identical monomers which are related to each other by a rotation of 177.6° along the non-crystallographic twofold axis. The large hydrophobic side chain also caused a rearrangement of the domain structure as demonstrated in Table 4. The root-mean-square deviations of C^{α} atoms between the A172L and A172F mutant structures are 0.31 Å for one subunit and 0.28 Å for the other. Small domain twist angles were found, 1.65° for one subunit and 0.83° for the other, between the two mutant enzymes.

Fig. 5 depicts the superimposed structure of A172F and A172L surrounding the mutation site. All the side chains are very similar except for the side chain of His300, which is the closest residue to site 172 on the opposite domain. The difference is ascribed to the different size of the side chains of the substituted residues. The distances between C^{α} atoms of residues 172 and 300 are 7.45, 7.56, 7.52, 9.68/9.17 and 10.0/9.23 Å when the site 172 residue is Gly, Ala, Val, Leu and Phe, respectively. Obviously, when the side chain is enlarged this distance increases greatly. As well as the rearrangement of domain structure, local main-chain movement and adjustment of the side chains were also found in the mutant enzymes with large side-chain residues at the mutation site. When A172F was superimposed on 10T to fold the protein backbone atoms of the first turn of the helix formed by residues 159–173 with each other, the C^{α} atom of residue 172 was shifted along the helices by 0.57 Å. The shift of residue 300 was calculated to be 0.49 Å from fitting the first turn of helix formed by residues 288–302. Owing to the location of both residues 172 and 300 on the helices, their C^{β} atoms are constrained at a certain position relative to the main-chain atoms; side chains were adjusted mainly by rotating their $C^{\alpha}-C^{\beta}$ and $C^{\beta}-C^{\gamma}$ bonds, as shown in Table 5.

3.5. Molecular-modelling study of the mutants substituted with Glu and Asp

Because of its poor diffracting power, the structure of A172E was not solved. Based on the structures of the wild-type and mutant enzymes, the three-dimensional structures of A172E and A172D were built using the molecular-modelling method. The lattice changes during crystallization described in §2 are ascribed to the conformational variation of the mutant enzymes in solution. As observed in the

Table 4
Comparison of structures between two mutant molecules of A172F and the native molecule.

Molecule	Fitting part	Twist (°)	Shift (Å)	R.m.s.d. of C^{α} atoms (Å)
Subunit 1	Entire molecule			1.86
	Domain 1			0.45
	Domain 2	10.1	13.5	0.51
Subunit 2	Entire molecule			1.06
	Domain 1			0.55
	Domain 2	1.2	10.4	0.33

Table 5
Dihedral angles (°) along the bonds $C^{\alpha}-C^{\beta}$ and $C^{\beta}-C^{\gamma}$ of the residues 172 and 300 in the mutant enzymes A172L and A172F.

Molecule	Position	Dihedral angle	A172F	A172L	Difference
Subunit 1	172	$N-C^{\alpha}-C^{\beta}-C^{\gamma}$	−90.0	−102.2	10.2
	172	$C^{\alpha}-C^{\beta}-C^{\gamma}-C^{\delta}$	80.2	18.8	61.4
	300	$C-C^{\alpha}-C^{\beta}-C^{\gamma}$	166.4	164.5	1.9
	300	$C^{\alpha}-C^{\beta}-C^{\gamma}-C^{\delta 2}$	−61.1	−86.7	25.6
Subunit 2	172	$N-C^{\alpha}-C^{\beta}-C^{\gamma}$	−78.4	−88.1	9.7
	172	$C^{\alpha}-C^{\beta}-C^{\gamma}-C^{\delta 1}$	73.6	39.3	34.3
	300	$C-C^{\alpha}-C^{\beta}-C^{\gamma}$	179.3	159.7	19.6
	300	$C^{\alpha}-C^{\beta}-C^{\gamma}-C^{\delta 2}$	−46.5	−72.2	25.7

structure of A172L and A172F, the different conformation may be caused solely by a different arrangement of domain structure. The shape of the type I crystal is very similar to those of other mutant enzymes crystallized from ammonium sulfate solution, such as the wild-type enzyme, A172G and A172V. Therefore, the conformation of the type I crystal is proposed to be similar to that of the wild type and the structure of the wild-type enzyme was chosen as the initial model. The structural analyses of other mutant enzymes showed that even the enzyme adopted a different conformation, its local structure changing slightly; hence, in the structure refinement of the model molecule all atoms inside the 6 Å sphere centred at residue 172 were restrained and the others were fixed as mentioned in §2.

Fig. 6 depicts the local structure around position 172 of the A172D and A172E mutant enzymes. Although the side-chain structures of Asp and Glu are very similar, the longer side chain by one C atom helps the carbonyl group of Glu to locate at a suitable distance to form a salt bridge with the side chain of Lys175, which confers the extra thermal stability on A172E. Meanwhile, two C atoms (C^{β} and C^{γ}) of Glu are located in the hydrophobic cavity. Therefore, glutamate contributes to the enzyme thermostability both by hydrophobic interactions with the internal surroundings and by forming an extra salt bridge on the protein surface, which is why A172E has a large deviation from the stability–hydrophobicity correlation, as shown in Fig. 1. In contrast, the side chain of Asp is located inside the cavity and the buried charge has a very destabilizing effect on the structure, as observed in other cases (Daopin, Anderson *et al.*, 1991; Moriyama *et al.*, 1995).

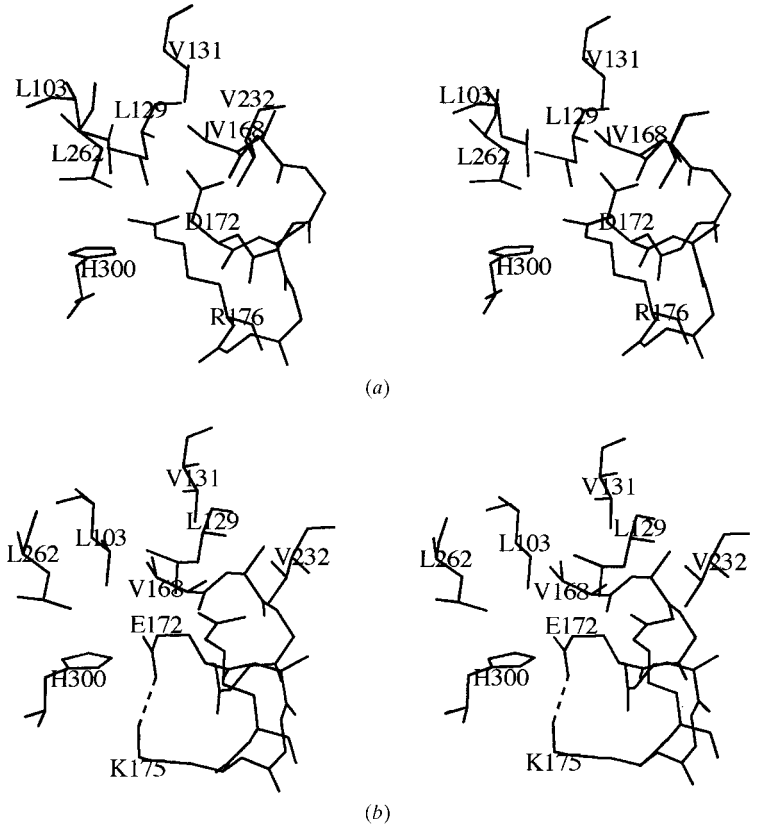

Figure 6
Local structures of the mutant enzymes A172D (*a*) and A172E (*b*), showing the interactions between the side chains of aspartic acid or glutamic acid and their neighbouring surroundings. The two models were built using *QUANTA*. The salt bridge formed between Glu172 and Lys175 is indicated by a dashed line. This figure was drawn using *MOLSCRIPT* (Kraulis, 1991).

4. Conclusions

4.1. Sequence conservation of the mutation site

Present analysis demonstrates that the position at 172 can accept multiple residue substitutions, even though it is a buried residue. As described in §1, the mutation site was found by the molecular evolutionary method; therefore, the multiple sequence alignment was performed on the IPMDH sequences derived from protein identification resources (PIR). As shown in Fig. 7, Ala is not conserved among the IPMDH sequences and other residues such as leucine, threonine, serine and methionine also appear at this site.

4.2. Thermostability of mutant enzymes and hydrophobicity of substituted residues

The energetic contribution to enzyme stability from amino acids at the mutation site Ala172 is mainly a consequence of the hydrophobic effect and the enzyme stability is correlated with the hydrophobicity of the substituted residues, as shown in Fig. 1. In cases

Table 6
Residues included the hydrophobic cores in the wild-type structure.

Type: one-letter amino-acid code. Sec: secondary structure; H and E represent α-helix and β-strand, respectively.

(*a*) Core 1.

Number	6	18	22	23	26	61	66	67	69	93	99	260	268	269
Type	L	A	V	L	L	V	A	V	L	L	L	A	V	F
Sec.	E	H	H	H	H	H	E	E	E	H	E	E	E	E
Number	291	294	295	297	298	311	314	315	318	319	336	340	344	
Type	I	A	A	M	L	V	A	V	A	L	F	V	L	
Sec.	H	H	H	H	H	H	H	H	H	H	H	H	H	

(*b*) Core 2.

Number	103	128	129	130	131	162	165	166	169	170	173	180	195	198
Type	L	V	L	I	V	V	V	A	A	F	A	V	W	T
Sec.	E	E	E	E	E	H	H	H	H	H	H	E	H	H
Number	199	232	233	234	243	247								
Type	V	V	V	V	L	A								
Sec.	H	E	E	E	H	H								

such as A172G and A172V, the differences in the packing of the local side chains are distinct. The cavity around the mutation site was detected using the program *QUANTA* (Molecular Simulation Inc.). Two parts of the cavity around the Ala172 C^{β} (Qu *et al.*, 1997) are connected by removing the C^{β} atom in the structure of A172G and are filled by adding two C^{γ} atoms in the structure of A172V. Therefore, in the structure of A172V there is no space for solvent molecules, which are conserved in both the wild-type and the A172G structures. In cases such as A172L and A172F, rearrangement of domain structures is observed and local packing becomes tighter. The hydrophobic contribution to the protein stability is made not only by buried side chains, but also by the main-chain movement which causes the local packing to be more tight, as demonstrated by Qu *et al.* (1997).

Bcal	167	EIERIVRMAFE**L**ARGRRK--	184
Bs	168	EIERVIREGFK**M**AATRKG--	185
Cb	167	EVERITRMAAF**L**SLQNDPPL	186
Pj	165	EVQRITRMAAF**M**ALQHNPPL	184
Bcoa	166	EIERIIEKAFQ**L**AQIRRK--	183
Tf	166	EIRRIAHVAFR**A**AQGRRK--	183
Ec	171	EIERIARIAFE**S**ARKRRH--	188
Taqu	161	EVERVAKVAFE**A**ARKRRR--	178
Tt	161	EVERVARVAFE**A**ARKRRK--	178
Bran	209	EIDRIARVAFE**T**ARKRRG--	226

Figure 7
The sequence alignment of IPMDHs obtained from protein identification resources (PIR). Bcal, *Bacillus caldotenax* (A26447); Bs, *B. subtilis* (A26522); Cb, *Candida boidinii* (A43324); Pj, *Pichia jadinii, Candida utilis* (A47620); Bcoa, *B. coagulans* (A24537); Tf, *Thiobacillus ferro-oxidans* (JX0286); Ec, *E. coli* (S40587); Taqu, *Thermus aquaticus* (JX0173); Tt, *T. thermophilus* (S41223); Bran, *Brassica napus* (S20510). The accession number of each entry is given in parentheses.

Although the enzyme stability is correlated with the hydrophobicity of the substituted residue, the mutational effect is dependent on the structural context of the mutation site, as shown in other cases (Zhang *et al.*, 1996). Local propensity can affect protein stability (Dill, 1990). However, the structure of the A172G mutant enzyme is stabilized by a salt bridge crossing the mutation site and by a water molecule. The effect of the salt bridge on protein stability has also been suggested by molecular modelling. Situated at a suitable position, the glutamic acid residue causes the formation of a salt bridge Glu172–Lys175 on the protein surface, while its in-cavity C atoms make favourable hydrophobic interactions with the cavity-forming residues.

The effect of replaced residues on the solvent-accessible surface area of the molecule can be calculated with the program *QUANTA*, using a 1.4 Å probe rolling on the protein surface. The values are 6819, 6820/6774, 6778 and 6774 Å^2 for the wild type, A172F, A172V and A172G, respectively. Although the thermal stability of the protein is reported to be related to the change in the solvent-accessible surface area on the mutation of one residue (Takano, Yamagata *et al.*, 1997), the present enzyme does not change its total area owing to the mutation at residue 172 because it maintains a concrete domain structure; the relative orientation of the domains is the only difference between the mutants. The change in the

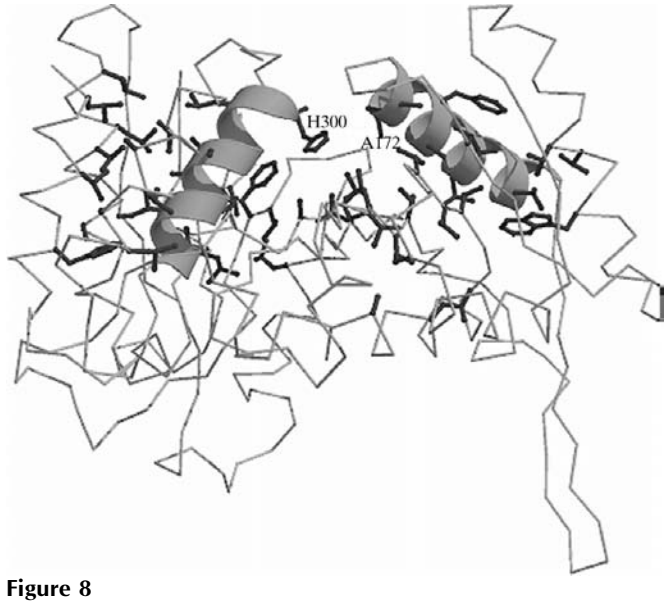

Figure 8
A diagram showing the hydrophobic cores of the wild-type enzymes. The side chains of core residues listed in Table 5 are depicted and the two helical ribbons represent the helices on which Ala172 and His300 are located.

exposed surface at residue 172 from the extended conformation (0, 8/6, 1 and 4% for the wild type, A172F, A172V and A172G, respectively) is almost zero, which shows the thermal stability does not correlate with its exposure.

4.3. Domain movements

Of particular interest is that the structure may accept large side chains into the cavity through a rearrangement of its domain structure, as observed in the cases of A172L and A172F mutants. The interaction between the side chains of residues 172 and 300 is a cause of the domain movements, which can be understood more clearly from the view of the packing of protein hydrophobic cores. The hydrophobic cores of the wild-type structure were detected using the program of Swindells (1995). Two hydrophobic cores were observed corresponding to the two domains in the structure. The residues involved in the hydrophobic cores and their secondary structures are listed in Table 6. As mentioned above, residue 172 is located on the helix formed by residues 159–173 and residue 300 is located on the helix formed by residues 288–302, as shown in Fig. 8. Both residues are not core residues, but are located on the inner surface of the domain cleft facing each other (Fig. 8). Five out of 27 and six out of 20 residues in the two hydrophobic cores (Table 6) are from these two helices. Therefore, the interactions between the side chains of these two residues cause the movement of the two helices as well as the two domains.

The present work was supported in part by a Grant-in-Aid for Scientific Research from the Ministry of Education, Science and Culture of Japan (Nos. 10044095 and 10179205). The authors thank Dr M. B. Swindells, Molecular Design Department, Yamanouchi Pharmaceutical Co. Ltd, Japan for his help in detecting the hydrophobic cores of the wild-type structure.

References

Akanuma, S., Qu, C., Yamagishi, A., Tanaka, N. & Oshima, T. (1997). *FEBS Lett.*, **410**, 141–144.
Akanuma, S., Yamagishi, A. & Oshima, T. (1995). *Protein Eng.* **8**, *Suppl.* 4.
Baldwin, E. P. & Matthews, B. W. (1994). *Curr. Opin. Biotech.* **5**, 396–402.
Brünger, A. T., Krukowski, A. & Erickson, J. (1990). *Acta Cryst.* A**46**, 585–593.
Daopin, S., Alber, T., Baase, W. A., Wozniak, J. A. & Matthews, B. W. (1991). *J. Mol. Biol.* **221**, 647–667.
Daopin, S., Anderson, D. E., Baase, W. A., Dahlquist, F. W. & Matthews, B. W. (1991). *Biochemistry*, **30**, 11521–11529.
Declerck, N., Joyet, P., Trosset, J.-Y., Garnier, J. & Gaillardin, C. (1995). *Protein Eng.* **8**, 1029–1037.
Dill, K. A. (1990). *Biochemistry*, **29**, 7133–7155.
Eriksson, A. E., Baase, W. A., Zhang, X. J., Heinz, D. W., Blaber, M., Baldwin, E. P. & Matthews, B. W. (1992). *Science*, **255**, 178–183.
Hurley, J. H., Baase, W. A. & Matthews, B. W. (1992). *J. Mol. Biol.* **224**, 1143–1159.
Imada, K., Sato, M., Tanaka, N., Katsube, Y., Matsuura, Y. & Oshima, T. (1991). *J. Mol. Biol.* **222**, 725–738.
Ishikawa, K., Nakamura, H., Morikawa, K. & Kanaya, S. (1993). *Biochemistry*, **32**, 5566–5575.
Iwasaki, Y. H., Numata, K., Yamagishi, A., Yutani, K., Sakurai, M., Tanaka, N. & Oshima, Y. (1996). *Protein Sci.* **5**, 511–516.
Jones, T. A. (1985). *Methods Enzymol.*, **115**, 157–171.
Kellis, J. T. Jr, Nyberg, K. & Fersht, A. R. (1989). *Biochemistry*, **28**, 4914–4922.
Kellis, J. T. Jr, Nyberg, K., Sali, D. & Fersht, A. R. (1988). *Nature (London)*, **333**, 784–786.
Kotsuka, T., Akanuma, S., Tomura, M., Yamagishi, A. & Oshima, T. (1996). *J. Bacteriol.* **178**, 723–727.
Kraulis, P. (1991). *J. Appl. Cryst.* **24**, 946–950.
Kunkel, T. A., Roberts, J. D. & Zakour, R. A. (1987). *Methods Enzymol.* **154**, 367–382.
Lim, W. A. & Sauer, R. T. (1991). *J. Mol. Biol.* **219**, 359–376.
Matsumura, M., Becktel, W. J. & Matthews, B. W. (1988). *Nature (London)*, **334**, 406–410.
Matsumura, M., Wozniak, J. A., Dao-pin, S. & Matthews, B. W. (1989). *J. Biol. Chem.* **264**, 6059–16066.
Moriyama, H., Onodera, K., Sakurai, M., Tanaka, N., Kirino-Kagawa, H., Oshima, T. & Katsube, Y. (1995). *J. Biochem.* **117**, 408–413.
Numata, K., Muro, M., Akutsu, N., Nosoh, Y., Yamagishi, A. & Oshima, T. (1995). *Protein Eng.* **8**, 39–43.
Onodera, K., Sakurai, M., Moriyama, H., Tanaka, N., Numata, K., Oshima, T., Sato, M. & Katsube, Y. (1994). *Protein Eng.* **7**, 453–459.
Qu, C., Akanuma, S., Moriyama, H., Tanaka, N. & Oshima, T. (1997). *Protein Eng.* **10**, 45–52.
Sakurai, M., Moriyama, H., Onodera, K., Kadono, S., Numata, K., Hayashi, Y., Kawaguchi, J., Yamagishi, A., Oshima, T. & Tanaka, N. (1995). *Protein Eng.* **8**, 763–767.
Sakurai, M., Onodera, K., Moriyama, H., Matsumoto, O., Tanaka, N., Numata, K., Imada, K., Sato, M., Katsube, Y. & Oshima, T. (1992). *J. Biochem.* **112**, 173–174.
Sandberg, W. S. & Terwilliger, T. C. (1989). *Science*, **245**, 54–57.
Sato, M., Yamamoto, M., Imada, K., Katsube, Y., Tanaka, N. & Higashi, T. (1992). *J. Appl. Cryst.* **25**, 348–357.
Shortle, D., Stites, W. E. & Meeker, A. K. (1990). *Biochemistry*, **29**, 8033–8041.
Swindells, M. B. (1995). *Protein Sci.* **4**, 93–102.
Takano, K., Funasaki, J., Yamagata, Y., Fujii, S. & Yutain, K. (1997). *J. Mol. Biol.* **274**, 132–142.
Takano, K., Ogasahara, K., Kaneda, H., Yamagata, Y., Fujii, S., Kanaya, E., Kikuchi, M., Oobatake, M. & Yutani, K. (1995). *J. Mol. Biol.* **254**, 62–76.
Takano, K., Yamagata, Y., Fujii, S. & Yutani, K. (1997). *Biochemistry*, **36**, 688–698.
Yamada, T., Akutsu, N., Miyazaki, K., Kakinuma, K., Yoshida, M. & Oshima, T. (1990). *J. Biochem.* **108**, 449–456.
Yutani, K., Ogasahara, K., Tsujita, T. & Sugino, Y. (1987). *Proc. Natl Acad. Sci. USA*, **84**, 4441–4444.
Zhang, H., Skinner, M. M., Sandberg, W. S., Wang, A. H.-J. & Terwilliger, T. C. (1996). *J. Mol. Biol.* **259**, 148–159.